ELSEVIER

Catalysis Today 38 (1997) 459–466

CATALYSIS TODAY

Development of solid oxide fuel cells based on a $Ce(Gd)O_{2-x}$ electrolyte film for intermediate temperature operation

M. Sahibzada[b], B.C.H. Steele[a], K. Zheng[a], R.A. Rudkin[a], I.S. Metcalfe[b,*]

[a]*Department of Materials, Imperial College of Science, Technology and Medicine, London SW7 2BP, UK*
[b]*Department of Chemical Engineering and Chemical Technology, Imperial College of Science, Technology and Medicine, London SW7 2BY, UK*

Abstract

Initial tests have been carried out with the fuel cell arrangement $La_{0.6}Sr_{0.4}Co_{0.2}Fe_{0.8}O_3||Ce_{0.9}Gd_{0.1}O_{1.95}||Ni/YSZ$, incorporating dense film (5–10 μm) $Ce_{0.9}Gd_{0.1}O_{1.95}$ electrolyte tape cast onto the supporting anode, to investigate the feasibility of intermediate temperature operation (500–700°C). A good open circuit voltage of approx. 0.8 V was obtained at 550°C using moist hydrogen as the fuel. Slightly lower open circuit voltages were found at higher temperatures, which may have been caused by minor gas leakage and the electronic conductivity of the electrolyte. Power outputs in excess of 100 mW/cm^2 were obtained at 650°C, and the cell resistance was 0.8 Ω cm^2 at this temperature. This resistance, and the greater resistance at lower temperature, was predominantly due to the cathode according to AC impedance measurements. Experiments were also carried out at 600°C using direct methanol fuels at the anode; the maximum power output was approximately half of that obtained with hydrogen. © 1997 Elsevier Science B.V.

Keywords: Solid oxygen fuel cell; Methanol reforming; Electrocatalyst; Ceria electrolyte

1. Introduction

1.1. Background

Solid oxide fuel cells (SOFCs) are a particular type of fuel cells which incorporate a dense solid oxide electrolyte membrane exhibiting a high oxygen ion conductivity and a low electronic conductivity. For fuel cell operation, porous catalysts are deposited as electrodes on both sides of the oxide membrane. Oxygen reduction takes place at the cathode and the resulting ions pass through the electrolyte to the anode where oxidation of the fuel occurs. Conventional SOFCs incorporating yttria-stabilised zirconia (YSZ) as the electrolyte are operated in the temperature range of 900–1000°C. This places considerable constraints on the materials which can be used for interconnections (bi-polar plates) and construction. To overcome these problems, Steele [1–3] suggested that the combination of ceria based electrolytes and stainless steel bi-polar plates operating over the temperature range 500–700°C offers the most cost effective way forward for SOFCs operating on either natural gas or methanol fuels. Recently, excellent performance of single 5×5 cm cell structures incorporating self-supported $Ce(Gd)O_{2-x}$ electrolyte foils have been reported at 700°C [4] and 800°C [5]. In order to

*Corresponding author. Tel.: (44-171) 594-5604; Fax: (44-171) 594-5604; e-mail: ism1@ic.ac.uk

PII S0920-5861(97)00055-2

achieve reasonable power densities at lower temperatures, we are fabricating cells incorporating $Ce_{0.9}Gd_{0.1}O_{1.95}$ (CGO) films of $\leq 20\,\mu m$ thickness supported on an electrode. We have already shown that there is significantly less cell resistance at 650°C under a H_2 fuel with an anode-supported CGO film than with a thicker self-supported CGO plate [6]. This paper gives some results using the prototype cell with the anode as the electrolyte support. Experiments have been carried out at 550–650°C using a H_2 fuel. In view of possible applications for these fuel cells in electric motor vehicles, experiments have also been carried out using externally reformed and direct methanol fuels.

1.2. *Choice of materials for intermediate temperature SOFC applications*

Steele [7,8] has discussed the selection of SOFC components for operation in the three temperature regimes, 500–700°C, 700–900°C and 900–1000°C. 500–700°C operation is classified as 'intermediate temperature' relative to all types of fuel cells.

For intermediate temperature (500–700°C) SOFCs, only supported films ($\leq 20\,\mu m$ thick deposited on either the cathode or anode as a support) of $Ce_{0.9}Gd_{0.1}O_{1.95}$ (CGO) or $La_{0.9}Sr_{0.1}Ga_{0.8}Mg_{0.2}O_{3-x}$ (LSGM) electrolytes can satisfy design targets for the area specific resistivity of $0.15\,\Omega\,cm^2$. Although LSGM has a wider ionic domain than CGO electrolyte (meaning LSGM maintains a high ionic conductivity relative to electronic conductivity in reducing conditions on the anode side, as well as in oxidising conditions on the cathode side), optimised cathodes are not yet available for LSGM.

Both the anode and the cathode must exhibit thermal expansivities compatible with the electrolyte to prevent delamination during heat up. They should have high electronic conductivities and preferably high oxygen-ion conductivities (if an electrode is non-conductive to oxygen ions, the oxygen exchange between the electrode and electrolyte will only take place at the triple phase boundary between the gas/electrode/electrolyte). They must also be chemically stable in contact with the electrolyte, i.e., the presence of interfacial reactions resulting in the production of third phases can be detrimental to oxygen-ion exchange.

It has been demonstrated [8] that $La_{0.6}Sr_{0.4}Co_{0.2}Fe_{0.8}O_{3-x}$ (LSCF) cathodes are stable in contact with CGO (such Co-containing cathodes would not be suitable in contact with YSZ because of interfacial reactions) and can exhibit excellent electrocatalytic kinetics for the reduction of oxygen, and so this combination was selected for these initial investigations.

Anode materials should be good catalysts for hydrogen and hydrocarbon activation. The anode should not promote carbon deposition, which may be a problem with direct hydrocarbon fuels and with externally reformed fuels containing CO. Ni/YSZ anode substrates (supplied by ECN, The Netherlands) were selected because they are known technology as the anode material for higher temperature fuel cells and Ni is catalytically active for hydrogen activation. However, it was recognised that Ni/CGO anode would be more compatible with the present electrolyte and would probably provide superior kinetic performance at intermediate temperatures. Furthermore, at around 500°C and high current densities there is, thermodynamically, the possibility of nickel oxide formation. This would of course be detrimental to the performance of the cell. Finally, there is also a question about the activity of nickel for the internal reforming of methanol at intermediate temperatures; there may be more appropriate electrocatalysts such as Cu/ZnO.

2. Experimental

2.1. *Preparation of anode-supported cell*

The $Ce_{0.9}Gd_{0.1}O_{1.95}$ (CGO) electrolyte film was supported on the anode, Ni/YSZ. CGO (Seattle Speciality Ceramics) electrolyte was tape cast onto one side of a flat 1 mm thick×25 mm diameter NiO/YSZ disc (supplied by ECN and pre-sintered at 1400°C). The assembly was sintered at 1400°C for 3 h to form a dense impermeable CGO film of approx. 5–10 μm thickness. After this, the cathode material, $La_{0.6}Sr_{0.4}Co_{0.2}Fe_{0.8}O_3$ (LSCF) (prepared in house), was tape cast on top of the CGO thick film. The active cathode area was approx. $2.5\,cm^2$. The combined structure was then sintered at 1280°C for 4 h to form a good contact between the LSCF and the CGO.

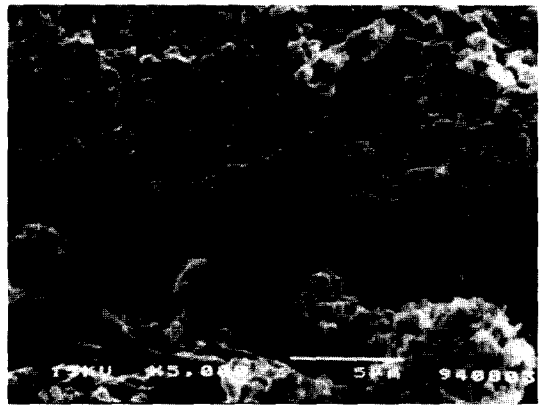

Fig. 1. SEM micrograph of the cross section of the LSCF||CGO (5–10 μm)||Ni/YSZ cell after 30 h operation under moist CO_2/H_2 fuel at 550–650°C.

During the cathode sintering process, two pieces of Pt mesh were also applied to the cathode and anode surface to act as current collectors. Electrical connections to the cell were made by spot welding Pt wires to the Pt mesh current collectors. The whole assembly was secured to the end of an AISI 446 alloy tube with glass sealant. The assembly was heated to the melting point of the glass sealant (850°C) for a short time to produce a gas impermeable seal.

The microstructure of the cathode/electrolyte/anode structure was examined by SEM. Fig. 1 shows an SEM micrograph of a cross section of a fuel cell after 30 h operation at 550–650°C under moist CO_2/H_2 fuel. The individual structural elements were found to exhibit good interfacial contact without signs of delamination. Highly porous electrodes were apparent, while the CGO electrolyte film was dense (>95% of theoretical density) with a thickness between 5 and 10 μm.

2.2. Current–voltage measurements

Two identical cells, prepared as in Section 2.1, were investigated in this study. Experiments with one cell assembly were carried out using moist CO_2/H_2 at 550–650°C, whereas the second cell was investigated with four different fuels at 600°C. Fig. 2 shows the experimental setup which was used to obtain current–voltage data. The cell assembly including the AISI 446 alloy cell holder was placed in a box furnace with the

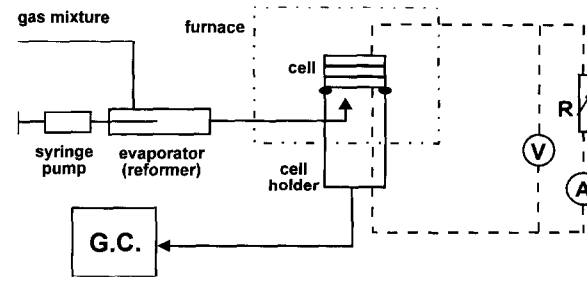

Fig. 2. Experimental apparatus used to obtain current–voltage measurements.

cathode exposed to air. The fuel was fed to the box furnace where it was heated to the set temperature before passing to the anode. The different fuels were made up as follows:

1. *Moist* CO_2/H_2. CO_2/H_2 (80% H_2, 20% CO_2) from a pre-mixed gas cylinder was fed by means of a mass flow controller through a room temperature water saturator. Hence the water partial pressure was approx. 3%, and the H_2 partial pressure was 77.5% (see Table 2). The moist CO_2/H_2 then passed to the cell. The total flow rate of this fuel was approximately 30 ml/min (STP).
2. *Reformed* CH_3OH/H_2O. An equimolar CH_3OH/H_2O liquid mixture was fed at a controlled rate from a syringe pump to a tubular evaporator/reactor, which was held at 250°C by means of a cylindrical furnace. After evaporation, the CH_3OH/H_2O passed over a $Cu/ZnO/Al_2O_3$ catalyst bed within the evaporator/reactor, producing CO_2/H_2 with approximately 90% yield. This was confirmed using a bypass line to the gas chromatograph, where it was found that the reformate composition was approximately 67.5% H_2, 22% CO_2, 6.5% H_2O, 2.5% CO (see Table 2). Similar results have also been found in other studies [9]. The flow rate of the CH_3OH/H_2O fuel was approx. 15 ml/min (STP) which would result in a flow rate of approx. 30 ml/min (STP) assuming complete reformation to CO_2 and H_2.
3. *Direct* CH_3OH/H_2O. A liquid mixture of CH_3OH/H_2O (85% CH_3OH, 15% H_2O) was fed at a controlled rate from a syringe pump to the tubular evaporator, which was held at 150°C. The evapo-

rated CH_3OH/H_2O then passed to the cell. The flow rate of this fuel was approx. 11 ml/min (STP), which would result in a flow rate of approx. 30 l/min (STP) assuming complete internal reforming of CH_3OH to CO/H_2.

4. *Direct* CH_3OH. CH_3OH was fed by the syringe pump through the tubular evaporator (150°C), and then to the cell. The flow rate of this fuel was approx. 10 ml/min (STP).

The resulting gas species were analysed by an ATI Unicam 610 series gas chromatograph. A Porapak column and a TCD detector allowed separation and analysis of CO, CO_2, CH_4, H_2O, and CH_3OH. The H_2 concentration in the product was calculated from an atomic balance to satisfy the C : H ratio in the feed.

The cell current and potentials were controlled by a Thompson Ministat precision potentiostat operating predominately in a galvanostatic mode. The open circuit voltage (OCV) increased very quickly (within a few minutes) to a steady value after first introducing the fuel to the anode side of the cell at the set temperature or after changing the temperature. The cell transients can be associated with the reduction of NiO. All current and voltage measurements given in this paper are the steady state results. The cell performance did not deteriorate over a period of many weeks (the cell performance was checked by periodically performing a standard test).

2.3. AC impedance spectroscopy

AC impedance spectroscopy measurements were carried out to identify the source of the cathode/electrolyte/anode cell resistance, and in particular to determine whether the resistance associated with the cathode formed a major part of the cell resistance. As such, symmetrical cells were fabricated with the cathode LSCF tape cast on either side of a pre-sintered dense self-supporting CGO electrolyte disc. The AC current output was measured with excitation potentials of <50 mV over a frequency range from 10 MHz to 10 mHz (generated by a Solartron FRA Model 1260). The corresponding electrode processes and analysis of such data have been well documented [10,11].

3. Results and discussion

3.1. Current–voltage measurements at 550–650°C using moist CO_2/H_2 fuel

Steady state OCV data at 550°C, 600°C and 650°C under the moist CO_2/H_2 fuel are given in Table 1. It can be seen that temperature increase had an adverse effect on the OCV. These OCV data were lower than those predicted by the Nernst Eq. (1) (the predicted OCV at 650°C is approx. 1 V). A minor amount of gas leakage through micropores in the CGO film (not seen by SEM) and more possibly through the glass edge seals may have caused some of the loss of OCV. Leakage of air to the fuel side was unlikely to take place, given that there was a slight positive pressure at the anode compared to the cathode, which was exposed to the air in the furnace. However, some fuel leakage to the air side may have taken place, which would lower the oxygen partial pressure and therefore lead to a lower cell EMF (1).

$$E = -(RT/4F)\ln(P'_{O_2}/P''_{O_2}), \quad (1)$$

where E is the cell EMF or OCV, F is Faraday's constant, P'_{O_2} the partial pressure of oxygen at the cathode and P''_{O_2} is the partial pressure of oxygen at the anode.

Another possible cause of the low OCV is that the CGO electrolyte is not a perfect ionic conductor, i.e it has a finite electronic conductivity in addition to the much greater ionic conductivity. Hence, under open circuit conditions there may be some short circuiting, i.e., a flux of electrons across the electrolyte from the anode to the cathode (and consequently a flux of O^{2-} ions from the cathode to the anode equal to half of the latter). The magnitude of the electronic flux is dependent upon the temperature and the electronic conductivity (itself related to the temperature) of the

Table 1
Anode-supported CGO film cell performace at 550–650°C under moist CO_2/H_2 fuel

Temperature (°C)	Open circuit voltage (V)	Area specific resistance (Ω cm^2)	Maximum power (mW/cm^2)
650	0.68	0.8	120
600	0.73	1.8	70
550	0.76	4.3	30

electrolyte, and is inversely related to the thickness of the electrolyte. This relationship is analogous to oxygen permeation in mixed conductors which are used for oxygen separation from air [12] (i.e., the oxygen ion and reverse electronic flux is related to the temperature, ionic conductivity, and inversely to the thickness of the electrolyte). Given that in the present study the thickness of the electrolyte was only 5–10 μm, the electronic flux (short circuiting current) under the open circuit conditions may have been significant. In this context we have shown previously [6] that the OCV at 650°C using moist CO_2/H_2 fuel was approximately 0.2 V greater for a cell incorporating self-supported (approx. 300 μm) CGO, than that for a cell incorporating the present dense film (5–10 μm) CGO. Given that the electronic flux is also related to the temperature, short circuiting may also account for the lower OCV observed at higher temperatures in the present study (Table 1).

Fig. 3 shows the current–voltage characteristics and the power density of the single cell at 550°C, 600°C and 650°C. The maximum cell power outputs obtained at the three temperatures are also given in Table 1. A power density of 120 mW/cm^2 was obtained at 650°C compared to 30 mW/cm^2 at 550°C. These cell power densities are encouraging for this prototype cell, but improvements could be made by reducing the cell internal resistance. It should be noted that these power outputs were obtained under conditions of excess fuel. In the worse case, at 300 mA/cm^2 (total current= 300 mA/cm^2×2.5 cm^2 cathode area=750 mA), the oxygen (O_2) flux through the electrolyte ($I/4F$ where I is the current and F is Faraday's constant) was

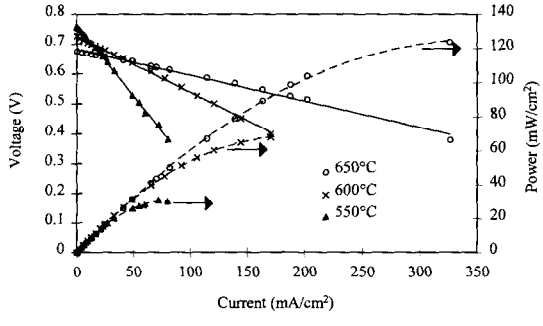

Fig. 3. Current–voltage performance of the anode-supported CGO film cell at 550–650°C under moist CO_2/H_2 fuel.

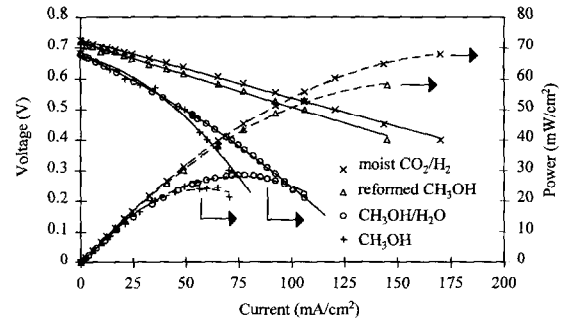

Fig. 4. Current–voltage performance of the anode-supported CGO film cell at 600°C under various fuels.

117 μmol/min or 2.6 ml/min (STP) compared to a H_2 flow of approx. 23 ml/min (STP). The linear current–voltage relationships in Fig. 3 indicate ohmic behaviour, and the cell resistances can be calculated from the gradients (see Table 1). The total cell resistance was 0.8 Ω cm^2 at 650°C compared to 4.3 Ω cm^2 at 550°C. AC impedance spectroscopy measurements were performed (described in Section 3.3) to identify the major component of this cell resistance.

3.2. *Current–voltage measurements at 600°C using various fuels*

Fig. 4 shows the current–voltage and the current–power profiles of the anode-supported CGO film fuel cell at 600°C under moist CO_2/H_2 (as above), under steam reformed CH_3OH, under direct CH_3OH/H_2O, and under direct CH_3OH. The performance of the cell under these fuels can be explained with reference to the concentration of H_2 which the anode was exposed to. The anode would be exposed to a concentration gradient from the fuel feed inlet to the product gas outlet as a result of reaction of the fuel. The feed and product gas chromatographic analyses are given in Table 2 (in order to provide a basis for comparison with the different fuels, all the product gases used in each analysis were obtained with a cell current of 175 mA). The average (feed to product) H_2 concentration was 68% in the case of moist CO_2/H_2, compared to 59% in the case of externally reformed CH_3OH, which is in line with the greater cell resistance (measured from the gradient of the current–voltage profile in Fig. 4) under the latter fuel. Further-

Table 2
Gas phase concentrations of fuel feed to the anode and the product effluent obtained from experiments at 600°C with a current of approximately 175 mA (70 mA/cm^2×2.5 cm^2)

Fuel	Feed fuel concentration							Product effluent concentration					
	H_2 (%)	CO_2 (%)	CH_3OH (%)	H_2O (%)	CO (%)	CH_4 (%)	O:C	H_2 (%)	CO_2 (%)	CO (%)	H_2O (%)	CH_4 (%)	O : C
Moist CO_2/H_2	77.5	19.5	—	3	—	—	2.15	59	15	2.5	19	3	2.51
Reformed CH_3OH[a]	67.5	22	—	6.5	2.5	1	2.04	51	18.5	3.5	21	4.5	2.32
CH_3OH/H_2O	—	—	85	15	—	—	1.18	48.5	8	20.5	14	8	1.38
CH_3OH	—	—	100	—	—	—	1.00	46	6	24	12	10	1.20

[a]The original feed fuel concentration before reforming was 50% CH_3OH and 50% H_2O and the corresponding atomic ratio O : C was 2.

more, the prevalent hydrogen concentrations are in line with the maximum power outputs of approx. 70 mW/cm^2 with moist CO_2/H_2, compared to approx. 60 mW/cm^2 with reformed CH_3OH.

The average (feed to product) H_2 concentrations were much less in the case of the direct CH_3OH/H_2O and pure CH_3OH fuels, 24% and 23% respectively. This would explain the inferior cell performance under these fuels. The maximum cell power outputs, approx. 30 and approx. 25 mW/cm^2, respectively, were approximately half of those found for the reformed fuel. The lower H_2 partial pressures would also result in lower rates of mass transfer to the anode and hence lower anodic limiting currents. Fig. 4 provides evidence for limiting currents in the case of the CH_3OH containing fuels, since the cell resistances (i.e., the gradients of the current–voltage profiles) appear to increase at high currents.

Note that in the case of the direct CH_3OH fuels, only trace CH_3OH was detected in the product, which would indicate that the Ni anode at 600°C was an active catalyst for internal reforming. This brings into question whether the anode was exposed to a concentration gradient of H_2 from the feed (0%) to the product, or whether the effective H_2 concentration was higher since the CH_3OH was rapidly reformed upon contact with the anode. It is worth noting that, although at 600°C complete reforming of the methanol took place, at a slightly lower temperature of 550°C (results not shown in this paper) the reforming was not complete, with approx. 40% CH_3OH being detected in the product. Therefore it is considered that in the present experiments at 600°C the effective H_2 concentration for the direct methanol fuels was lower than that for the reformed fuels. It follows that an improvement in the performance of the cell under direct CH_3OH fuels may be possible by combining a more active reforming catalyst, such as ZnO, with the existing Ni anode.

It is interesting that CH_4 formation at the anode was greater in the case of the direct CH_3OH/H_2O or CH_3OH fuel compared to moist CO_2/H_2 or reformed CH_3OH fuel (see Table 2). This suggests that CH_4 is produced over Ni directly from CH_3OH or from the CO which is produced from the internal reforming of CH_3OH (see Table 2).

Table 2 also shows the overall O : C atomic ratio in the products compared to that in the feed fuel. This data is useful to determine how much additional oxygen was derived electrochemically (as discussed previously in Section 3.1, additional oxygen was unlikely to have come from air leakage to the anode side). In all cases the product O : C ratio was greater in the product than in the feed. In the case of the direct CH_3OH fuel, the 1.2 O : C ratio for the product stream indicates a 20% excess of atomic oxygen. Given that the CH_3OH feed flow was approx. 10 ml/min (STP) or 450 μmol/min, the excess atomic oxygen in the product was approx. 90 μmol/min. With the current at 175 mA (70 mA/cm^2×2.5 cm^2), the corresponding oxygen ion (O^{2-}) flux (given by $I/2F$) was 55 μmol/min. The remaining approx. 35 μmol/min atomic oxygen was probably a result of oxygen ion permeation due to the finite electronic conductivity. As discussed previously in Section 3.1, the oxygen ion (and reverse electronic) permeation may have been significant in the present study due to the thickness of the electrolyte being only 5–10 μm.

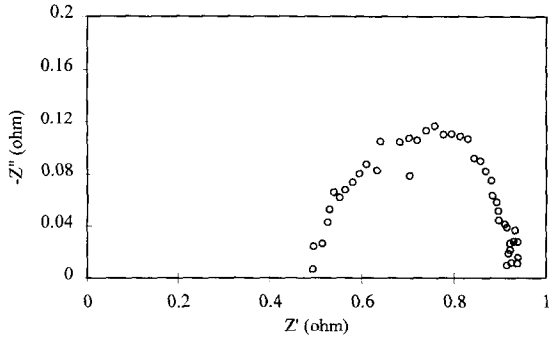

Fig. 5. AC impedance spectroscopy of symmetrical cell LSCF||CGO (approx. 300 μm)||LSCF at 650°C.

3.3. AC impedance spectroscopy

AC impedance spectroscopy was carried out to resolve which interface or component of the cell contributed most to the cell resistances as given in Table 1. Fig. 5 shows a typical result at 650°C using a symmetrical cell with the LSCF cathode applied to either face of a dense self-supported CGO disc. Relaxation processes give rise to an impedance spectrum described by the arc. The electrode polarisation resistance is then the difference between the high and low frequency intercepts with the real axis [10,11]. From Fig. 5 it can be calculated that the resistance associated with the cathode is $0.45\ \Omega \times 2.5\ cm^2/2 = 0.56\ \Omega\ cm^2$, given that the electrode has two parallel faces with an equivalent area of $2.5\ cm^2$ each. Therefore the cathode resistance forms the major part of the $0.8\ \Omega\ cm^2$ total cell resistance found at 650°C (Table 1). The cathode contributed to a similar proportion of the total cell resistance at lower temperatures, and more detailed AC impedance data can be found elsewhere [13,14]. From this analysis, it is suggested that the performance of the cell is limited by the cathode.

In other works it has been found that etching the CGO surface to remove impurities and applying LSCF as a bi-layer, incorporating a dense layer to improve oxygen exchange with the electrolyte and a second porous layer, reduces the resistance associated with the cathode by an order of magnitude [13]. The fabrication of a cell with this improved cathode structure is currently underway.

4. Conclusions

This paper shows that an electrode-supported CGO film is a suitable basis for intermediate temperature (550–650°C) operation of fuel cells. Power densities in excess of $100\ mW/cm^2$ at 650°C and $30\ mW/cm^2$ at 550°C have been obtained under a H_2-containing fuel. Approximately half as much power is obtainable under direct CH_3OH fuels. Future work will focus on improving the performance of the anode for the internal reforming of direct methanol fuels and particularly on improving the performance of the cathode (in terms of oxygen activation at the surface and interfacial contact with the electrolyte) which is associated with most of the resistance of the present cell.

Acknowledgements

This work was carried out with financial support from the EPSRC. We are grateful to ECN, The Netherlands, for providing the Ni/YSZ cermet used in the present investigation.

References

[1] B.C.H. Steele, J. Power Source 49 (1994) 1.
[2] B.C.H. Steele, in: U. Bossel (Ed.), Proceedings of the First European Solid Oxide Fuel Cell Forum, ISBN 3-922-14-X, 1994, p. 375.
[3] B.C.H. Steele, Proceedings of the 1994 Fuel Cells Seminar, San Diego, CA, 1994.
[4] F.P.F. van Berkel, G.M. Christie, F.H. van Heuveln, J.P.P. Huijsmans, in: M. Dokiya, O. Yamamoto, H. Tagawa, S. Singhal (Eds.), Solid Oxide Fuel Cells IV, Electrochem. Soc., NJ, 1995, p. 1062.
[5] M. Godickemeier, K. Sasaki, L.J. Gaukler, I. Riess, Solid State Ionics 86–88 (1996) 691.
[6] K. Zheng, B.C.H. Steele, M. Sahibzada, I.S. Metcalfe, Solid State Ionics 86–88 (1996) 1241.
[7] B.C.H. Steele, Br. Ceram. Proc. 56 (1996) 151.
[8] B.C.H. Steele, Solid State Ionics 86 (1996) 1223.
[9] C.J. Jiang, D.L. Trimm, M.S. Wainwright, N.W. Cant, Appl. Catal. A 93 (1993) 245.
[10] J. Ross Macdonald, Impedance Spectroscopy, Wiley, New York, NY, 1987.
[11] J.E. Bauerle, J. Phys. Chem. Solids 30 (1969) 2657.
[12] J.E. ten Elshof, H.J.M. Bouwmeester, H. Verweij, Solid State Ionics 81 (1995) 97.

[13] J.A. Lane, P.H. Middleton, H. Fox, B.C.H. Steele, J.A. Kilner, in: T.A. Ramanarayanan, W.L. Worrell, H.L. Tuller (Eds.), Proceedings of the Second International Symposium on Ionic and Mixed Conducting Ceramics, Electrochem. Soc., NJ, 1995.

[14] M. Sahibzada, B.C.H. Steele, K. Zheng, R.A. Rudkin, J.M. Bae, N. Kiratzis, D. Waller, I.S. Metcalfe, in: B. Thorstensen (Ed.), Proceedings of the 2nd European Solid Oxide Fuel Cell Forum, Oslo, May 1996, Ulf Bossel, p. 687.